

# A New Procedure for Selecting and Ranking Ground-Motion Prediction Equations (GMPEs): The Euclidean Distance-Based Ranking (EDR) Method

by Özkan Kale and Sinan Akkar

**Abstract** We introduce a procedure for selecting and ranking of ground-motion prediction equations (GMPEs) that can be useful for regional or site-specific probabilistic seismic hazard assessment (PSHA). The methodology is called Euclidean distance-based ranking (EDR) as it modifies the Euclidean distance ( $DE$ ) concept for ranking of GMPEs under a given set of observed data.  $DE$  is similar to the residual analysis concept; its modified form, as discussed in this paper, can efficiently serve for ranking the candidate GMPEs. The proposed procedure separately considers ground-motion uncertainty (i.e., aleatory variability addressed by the standard deviation) and the bias between the observed data and median estimations of candidate GMPEs (i.e., model bias). Indices computed from the consideration of aleatory variability and model bias or their combination can rank GMPEs to design GMPE logic trees that can serve for site-specific or regional PSHA studies. We discussed these features through a case study and ranked a suite of GMPEs under a specific ground-motion database. The case study indicated that separate consideration of ground-motion uncertainty (aleatory variability) and model bias or their combination can change the ranking of GMPEs, which also showed that the ground-motion models having simpler functional forms generally rank at the top of the list. We believe that the proposed method can be a useful tool to improve the decision-making process while identifying the most proper GMPEs according to the specific objectives of PSHA.

*Online Material:* MATLAB script and sample input file for EDR index calculation.

## Introduction

Ground-motion prediction equations (GMPEs) are the main tools used in estimating ground-motion intensities for the purpose of assessing seismic hazard in a seismic-prone region. Recently, the increasing size and quality of the ground-motion databases have resulted in a significant number of new local and global predictive models. Consequently, engineering seismologists have begun to propose a number of statistical and probabilistic procedures to rank and select GMPEs to properly address the seismotectonic features of the region considered for hazard assessment. One of the major objectives of these efforts is to reduce the uncertainty in ground-motion variability that, essentially, affects the computed hazard at long return periods.

There are numerous methods in the statistical literature to test the agreement between observed and predicted data (e.g., chi-square test, Kolmogorov–Smirnov test, variance reduction, Pearson’s correlation coefficient, and Nash–Sutcliffe efficiency coefficient). Recently, these methods have been evaluated by various studies to understand the

suitability of a given predictive model under a set of collected ground motions (e.g., Scherbaum *et al.*, 2004; Kakkamanos and Baise, 2011). That said, the most common methodology for assessing predictive model performance remains as classical residual analysis. This statistical method determines the existence of bias through the application of mean residuals, as well as the slopes of the straight lines fitted to the various residual components (i.e., between-event, within-event, or total residuals) as functions of estimator parameters such as magnitude and source-to-site distance. Studies like Bindi *et al.* (2006), Scassera *et al.* (2009), and Shoja-Taheri *et al.* (2010) used residual analysis to evaluate GMPEs under different ground-motion databases. The recent likelihood-based testing and ranking techniques proposed in Scherbaum *et al.* (2004, 2009) as likelihood (LH) and log-likelihood (LLH) methods, respectively, have also appealed to the seismological and engineering communities as they are easy to implement with well-tailored outcomes to define the best performing GMPEs for a given ground-motion dataset. The

LH method calculates the normalized residuals for a set of observed and estimated ground-motion data. It assumes that predictive model residuals are log-normally distributed, and it calculates the exceedance probabilities of residuals as LH values. The suitability of candidate GMPEs is identified through the median LH value that is described as the LH index, which takes values between 0 and 1. For an optimum case, LH values are evenly distributed between 0 and 1, and the median of LH is  $\sim 0.5$ . The LLH method is an information-theoretic model selection procedure, and it is based on the log-likelihood approach to measure the distance between two continuous probability density functions,  $f(x)$  and  $g(x)$ . The distribution of  $f(x)$  that is supposed to exist for each individual data point in the observed ground-motion dataset is not known *a priori*. This method calculates the average log-likelihood of a predictive model whose distribution,  $g(x)$ , is known through its median and standard deviation sigma. The method computes the occurrence probability of the observed data point by using the probability distribution of the candidate GMPE. In this way, it computes the LLH value as the model selection index.

The LH method was initially applied to the broader region of France, Germany, and Switzerland for a small set of observed data (Scherbaum *et al.*, 2004). Later, Hintersberger *et al.* (2007) extended the dataset for the same region and implemented the same method using the same candidate GMPEs as that of the former study. These two studies obtained similar ranking results for the same set of candidate GMPEs, advocating the robustness of LH indices for selecting the proper GMPEs in hazard analysis. Stafford *et al.* (2008) evaluated the applicability of next generation attenuation (NGA; Power *et al.*, 2008) GMPEs to Euro-Mediterranean region by using LH, as well. This method was also considered in Kaklamanos and Baise (2011) as supplementary to the results of Nash–Sutcliffe model efficiency coefficient (Nash and Sutcliffe, 1970) to validate the NGA GMPEs by making use of a ground-motion dataset assembled from the recent earthquakes recorded in California. The information-theoretic LLH approach that supersedes the LH technique was used for the selection and ranking of GMPEs in various studies, as well (e.g., Delavaud *et al.*, 2009; Beauval *et al.*, 2012a,b; Delavaud, Cotton, *et al.*, 2012; Delavaud, Scherbaum, *et al.*, 2012; Mousavi *et al.*, 2012). Of these studies, the Delavaud, Cotton, *et al.* (2012) paper uses LLH as an adjunct tool to determine the logic-tree weights of the GMPEs that are used in assessing the hazard in Europe and south Mediterranean region under the framework of the Seismic Hazard HARMONIZATION in Europe (SHARE) project.

This study presents an alternative testing and ranking approach for a preselected set of GMPEs. Although the LH and LLH methods inspired us while working on our methodology, we used an approach different than those of the LH and LLH methods while considering the model bias and aleatory variability in the estimated ground motions. Our method uses the Euclidean distance: the absolute difference between the observed and estimated data (analogous to the

residual analysis concept) to account for the trend (model bias) between the observed and estimated ground-motion data. The method also employs Euclidean distance to account for aleatory variability in ground motions (addressed by the standard deviation of GMPE) through an approach similar to that of probabilistic seismic hazard assessment (PSHA). These two features, consideration of model bias and aleatory variability, make the method appealing for PSHA projects that carry different types of objectives (e.g., regional versus site-specific PSHA studies). The method presents ranking results that are normalized by the total number of data, which can be considered as an additional strength while selecting and ranking of GMPEs for regions of sparse data. The following sections first summarize a number of important observations on the most frequently used testing and ranking methodologies and then describe the fundamental concepts of our proposed method. The paper ends with a case study to show the practical implementation, as well as the specific features, of the proposed methodology. We believe that the proposed procedure can be used efficiently while identifying the proper suites of GMPEs for hazard studies of different objectives. However, we also believe that the sole use of our procedure for testing and ranking of GMPEs would be insufficient as a rigorous selection methodology should be an integral process that considers multiple statistical measures. The decision-making process could be improved significantly with the consideration of additional testing methods, as well as the conventional residual analysis that is especially helpful as a visual tool.

### Summary of Some Observations on the Current Testing and Ranking Methods

Scherbaum *et al.* (2004) studied simple statistical measures such as significance tests, variance reduction, and Pearson's correlation coefficient while proposing the LH method. In their paper, the authors indicated that these methods do not produce consistent outcomes to properly rank the performance of candidate GMPEs for a given ground-motion dataset. The direct implementation of conventional residual analysis, despite its visual efficiency in explaining the level of agreement between the median predictions and observed data (model bias), also will not provide flexible options for ranking candidate GMPEs. The model efficiency coefficient (Nash and Sutcliffe, 1970) is a major improvement over the goodness-of-fit statistics previously discussed because it directly quantifies the amount of bias in a model (Pearson's correlation coefficient, for example, is not sensitive to additive and multiplicative biases). However, it does not quantify how well the aleatory variability sigma of the observations is predicted by the models.

Although the LH method was proven to be a robust approach for ranking the candidate GMPEs, its dependence on data size and subjectivity in choosing the threshold LH value led Scherbaum *et al.* (2009) to propose the LLH method that overcomes these weaknesses. This method treats GMPEs

as probability distributions by means of their medians and standard deviations. Because of the specific features of the ground-motion dataset used in testing, this method may favor GMPEs with larger standard deviations as they can predict outlier observations with higher probabilities. Such a case can be observed, for example, during the testing of two GMPEs having fairly similar median estimations and different standard deviations. The LLH method can lead to better performance of the predictive model with larger sigma, in particular, if the observed data are accumulated away from the median estimations of the two GMPEs. Consistent with the underlying theory in LLH, the competing predictive model with larger sigma would yield larger probabilities of occurrence indicating that it can capture these outliers better than its alternative.

The previous discussions about LLH are illustrated by a case study as presented in Figure 1. Figure 1a,b shows ob-

served versus estimated peak ground acceleration (PGA) data in natural logarithms for two candidate GMPEs, Akkar and Çağnan (2010) and Özbey *et al.* (2004), that are designated as models A and B, respectively. The observed dataset is extracted from a strong-motion databank that is compiled for the Earthquake Model of the Middle East (EMME) project; detailed information about this databank is discussed in the latter sections of the paper. The scatter plot in the second row compares the median estimations of these two models for the same dataset, indicating almost identical median trends. The almost exact matching of median estimations of the two GMPEs is also verified by calculating the model efficiency coefficient,  $E$  (Nash and Sutcliffe, 1970). The  $E$  values from models A and B are the same (63%). The standard deviation of model A ( $\sigma_{\text{modelA}} = 0.832$ ) is larger than that of model B ( $\sigma_{\text{modelB}} = 0.599$ ). The LLH testing results of these GMPEs for models A and B are 1.91 and 2.21, respectively, for the

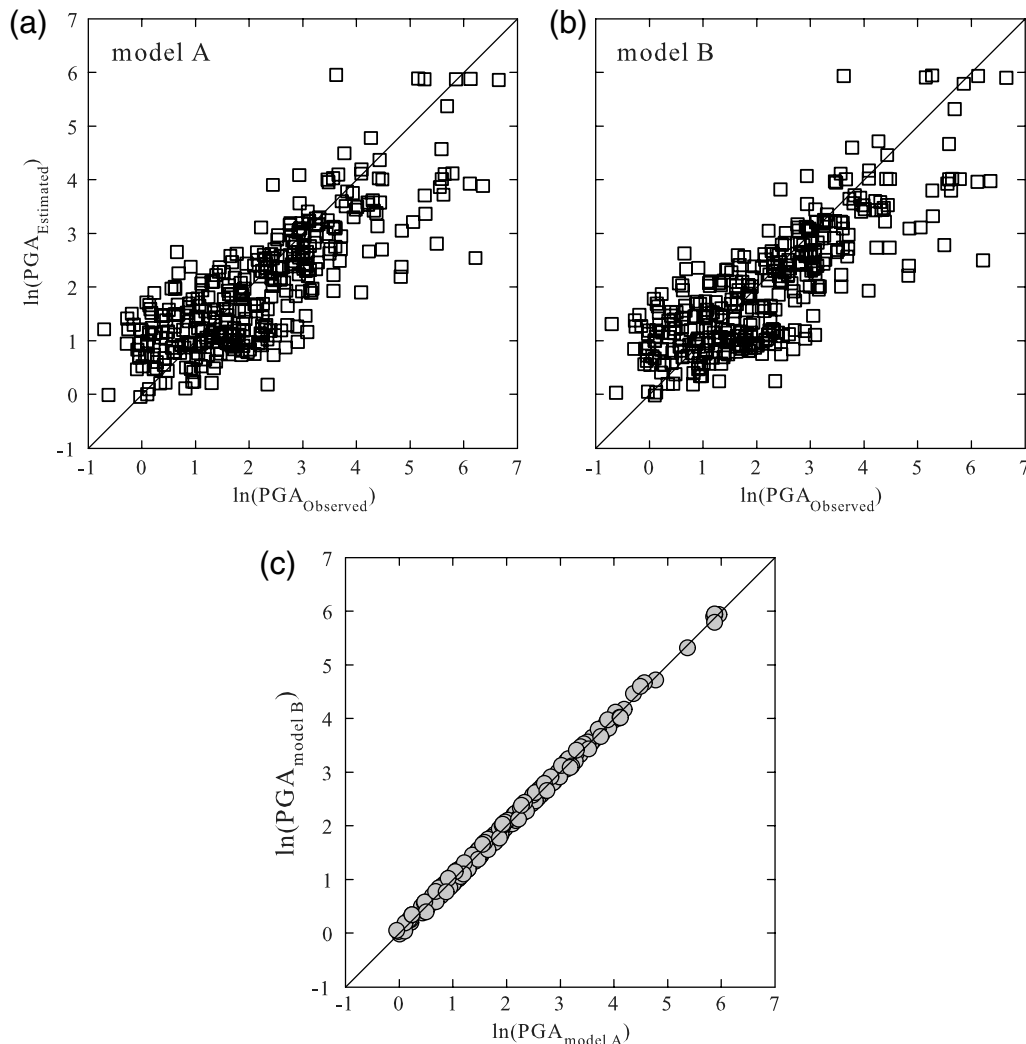


**Figure 1.** Natural logarithms of observed versus estimated peak ground acceleration (PGA) data corresponding to (a) models A and (b) B. Panel (c) shows scatter plot comparisons of the ground-motion estimations of these two models for the observed data. The sigma values of models A and B are 0.832 and 0.599, respectively.

given dataset. This indicates that LLH favors model A against the performance of B (smaller LLH values can be interpreted as the accurate description of aleatory variability posed by the ground-motion dataset). We note that, of the same GMPEs, the LLH method would have chosen the GMPE with smaller sigma if the observed data displayed a closer distribution to the median estimations of the considered GMPEs.

Discussions of the LLH method in the previous paragraphs indicate that this method (as well as its predecessor, the LH method) focuses on selecting a suite of GMPEs that can accurately represent the aleatory variability of the ground-motion dataset used in testing. As given in the previous case study, this objective may favor GMPEs with large sigma that may result in conservative probabilistic seismic hazard for long-return periods (Restrepo-Velez and Bommer, 2003). The proposed method provides an alternative approach to describe the aleatory variability featured by the ground-motion dataset. The dispersion of the ground-motion dataset and uncertainty of the estimations computed from the GMPE are considered together, which is achieved by computing the occurrence probabilities of differences between the observed data and a range of model estimations that are described for an interval of sigma values. Besides, the method accounts for model bias by using a factor computed from residual analysis. The method then combines these two separate effects as an index to rank the overall performance of GMPE. The effects of aleatory variability and model bias can also be considered separately depending on the specific purposes of the PSHA study. The derivation of the proposed method, as well as its specific properties, is discussed in the subsequent sections of this paper.

### Proposed Testing and Ranking Method

The highlighted observations on the likelihood methods, as well as other statistical measures, motivated us to present an alternative testing-and-ranking methodology that can lead to a practical and robust strategy for selecting the most appropriate set of GMPEs for a given ground-motion dataset. Our interpretation from background studies advocate that a versatile ranking-and-selection procedure should account for the influence of sigma on the estimated ground motions and measure the bias between the observed data and median estimations. In our opinion, these features are the central aspects for detecting a proper set of GMPEs to be used in PSHA that serve for different objectives, such as site-specific or regional studies. Moreover, the competency of the method should not be limited to the data size because obtaining large amounts of ground-motion data might not be possible for some seismic-prone regions.

We call our proposed methodology the Euclidean distance-based ranking (EDR) method as it uses the Euclidean distance ( $DE$ ) definition given in equation (1). Euclidean distance is a statistical index where the square root of a sum of squares of the differences between  $N$  data pairs ( $p_i, q_i$ ) is calculated. The parameters  $p_i$  and  $q_i$  in equation (1) desig-

nate the observed and estimated ground-motion data in our methodology. In the proposed ranking method, the  $DE$  definition is slightly modified considering some basic probability rules to account for the criteria mentioned in the previous paragraph. These modifications and the theory behind are discussed in the following subsections:

$$DE^2 = \sum_{i=1}^N (p_i - q_i)^2. \quad (1)$$

#### Consideration of Sigma: Uncertainty in Ground-Motion Estimations

While considering the influence of standard deviation sigma, an analogy is made from the implementation of GMPEs in PSHA. The GMPEs are used for a range of sigma values in PSHA to address the randomness in ground-motion estimations. In the proposed methodology, the estimated ground-motion intensity for a single data point (that consists of a certain magnitude, distance, style-of-faulting, and site class) is assumed to take a set of values that is computed from a predetermined range of standard deviation of the considered GMPE. In other words, for a single observed data point, the candidate GMPE can estimate a range of values due to the aleatory variability in ground motions. The differences between the observed data point and the range of estimations for that single point result in a probability distribution. Our procedure considers this distribution while assessing the performance of the candidate GMPE under the ground-motion dataset. The following paragraphs describe the background theory of this approach.

The EDR method assumes that the natural logarithm of the predictive model, as well as the Euclidean distances computed for each data point, is normally distributed. Let  $D$  in equation (2) denote the difference between the natural logarithms of an observed ( $a$ ) and estimated ( $Y$ ) data point. In this expression,  $a$  is scalar quantity (single observation) whereas  $Y$ , the estimator for a predictive model, is a Gaussian random variable with mean,  $\mu_Y$ , and variance,  $\sigma_Y^2$ . From the basic principles of the summation of random variables,  $D$  can be proven to be a normally distributed variety (Devore, 2004) with parameters given in equations 3a and 3b:

$$D = a - Y \quad (2)$$

$$\mu_D = a - \mu_Y \quad (3a)$$

$$\sigma_D^2 = \sigma_Y^2. \quad (3b)$$

For each single point, the square of  $D$  values contributing to  $DE$  are non-negative. If we seek to establish an analogy between  $D$  and  $DE$ , we must consider the probability

distribution of the absolute values of  $D$  [i.e.,  $\Pr(|D|)$ ]. Equation 4 shows the probability of  $|D|$  being less than a certain value  $d$  [i.e.,  $\Pr(|D| < d)$ ], which is actually the difference between  $\Pr(D < d)$  and  $\Pr(D < -d)$  as shown in Figure 2. The parameter  $\Phi$  denotes the normal cumulative distribution function in equation (4). This equation will be used to derive the probability distribution of  $|D|$ :

$$\begin{aligned} \Pr(|D| < d) &= \Pr(D < d) - \Pr(D < -d) \\ &= \Phi\left(\frac{d - \mu_D}{\sigma_D}\right) - \Phi\left(\frac{-d - \mu_D}{\sigma_D}\right). \end{aligned} \quad (4)$$

For discrete values of  $D$ , which are denoted by  $d_j$  in our terminology, the occurrence probability of  $d_j$  [i.e.,  $\Pr(d_j)$ ] is described within an infinitesimal bandwidth  $dd$  around  $d_j$  [i.e.,  $\Pr(d_j - dd/2 < D < d_j + dd/2)$ ]. As the method considers the occurrence probabilities of  $d_j$  through the analogy made between  $DE$  and  $D$ , we therefore modify this probability as  $\Pr(|D| < |d_j|)$ . Such a relationship can be derived by making use of equation (4), and it is given in equation (5). Figure 3 and its caption describe the meanings of each term in equation (5):

$$\begin{aligned} \Pr(|D| < |d_j|) &= \Pr\left(|d_j - \frac{dd}{2}| < |D| < \left|d_j + \frac{dd}{2}\right|\right) \\ &= \Pr\left(|D| < \left|d_j + \frac{dd}{2}\right|\right) - \Pr\left(|D| < \left|d_j - \frac{dd}{2}\right|\right). \end{aligned} \quad (5)$$

The total occurrence probability for a set of  $|d_j|$  values is called modified Euclidean distance (MDE) in our procedure. Equation (6) defines the discrete modified Euclidean distance ( $MDE_d$ ) when  $|D|$  is described in discrete points. In this equation,  $n$  is the number of discrete points that depends on the bandwidth of  $dd$  (Fig. 3c,d) and the maximum value of  $|d|$  (i.e.,  $|d|_{\max}$ ). If  $|D|$  is assumed to be continuous, the integral expression given in equation (7) is used to calculate the continuous modified Euclidean distance ( $MDE_c$ ):

$$MDE_d = \sum_{j=1}^n |d_j| \Pr(|D| < |d_j|) \quad (6)$$

$$\begin{aligned} MDE_c &= \int_0^{|d|_{\max}} d \times \frac{1}{\sqrt{2\pi} \times \sigma_D} \times \exp\left(\frac{-(d - \mu_D)^2}{2\sigma_D^2}\right) \times dd \\ &+ \int_0^{|d|_{\max}} d \times \frac{1}{\sqrt{2\pi} \times \sigma_D} \times \exp\left(\frac{-(-d - \mu_D)^2}{2\sigma_D^2}\right) \times dd. \end{aligned} \quad (7)$$

MDE can be considered as a probability-based average that is used as an index to account for the effect of sigma while testing the performance of GMPEs under a given ground-motion dataset (equations 6 and 7). The entire methodology is based on the Euclidean distance concept that is very similar to residual analysis. We preferred Euclidean distance instead of residual analysis, as it results in non-negative differences between observations and estimations that can be easily transformed into an index.

For practical applications of our method, we suggest that  $|d|_{\max}$  value should be selected in accordance with the following relationship:

$$|d|_{\max} = \max(|\mu_D \pm x \times \sigma_D|). \quad (8)$$

In equation (8),  $x$  denotes the multiplier of sigma and  $|d|_{\max}$  depends on the value of this parameter. If  $x$  is selected as 3, our procedure would approximately cover 99.7% of the differences between the observation and estimations of a candidate ground-motion model, provided that the normality assumption holds for the considered variables in the methodology. We note that the distribution of  $D$  is unsymmetrical about zero unless there is a one-to-one match between the observed data point and the corresponding median estimation. Conversely, the  $|d_j|$  pairs (i.e.,  $|d_j|$  and  $-|d_j|$ ) are always symmetric about zero. These remarks are illustrated in Figure 3c.

Table 1 provides an insight about the variation of MDE for a set of  $x$  and  $dd$  values by considering an arbitrary ground-motion model and a sample dataset. The MDE values are computed by considering the probability distribution of  $D$  either as discrete ( $MDE_d$ ) or continuous ( $MDE_c$ ). The results given in Table 1 are derived for  $\mu_D = 0.75$  and

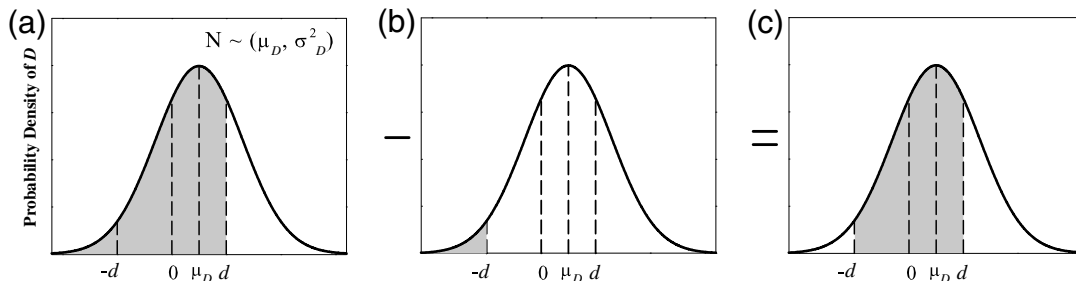


**Figure 2.** Probability distribution definitions given in equation (4): (a)  $\Pr(D < d)$ , (b)  $\Pr(D < -d)$ , and (c)  $\Pr(|D| < d)$ .

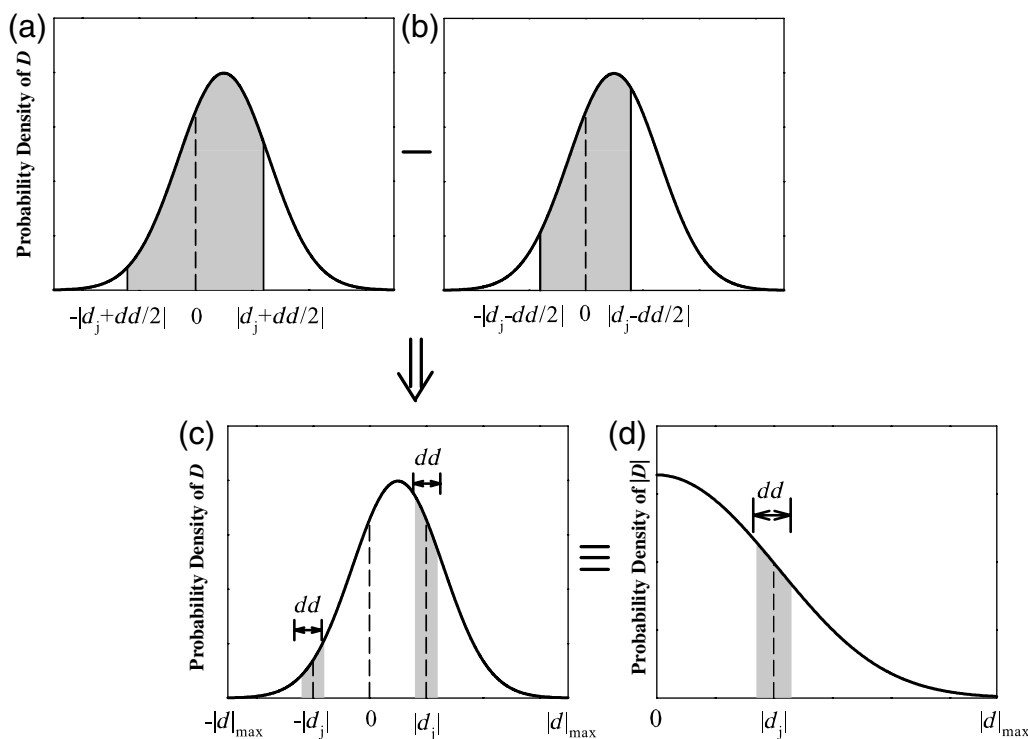


**Figure 3.** Probability distribution definitions given in equation (5): (a)  $\Pr(-|d_j + dd/2| < D < |d_j + dd/2|)$ ; (b)  $\Pr(-|d_j - dd/2| < D < |d_j - dd/2|)$ ; (c) difference between the probabilities given in (a) and (b); total discrete probability,  $\Pr(|D| < |d_j|)$ , and (d) probability density function of  $|D|$ . The probabilities of (a) and (b) are equivalent to  $\Pr(|D| < |d_j + dd/2|)$  and  $\Pr(|D| < |d_j - dd/2|)$ , respectively. The gray shaded area in (d) represents the summation of the discrete probabilities in negative and positive sides of the probability-density function in (c) [i.e.,  $\Pr(|D| < |d_j|)$ ].  $D$  is normally distributed random variable with  $\mu_D$  and  $\sigma_D^2$  while  $|D|$  is a non-negative random variable.

$\sigma_D = 0.5$ . They suggest that when  $x$  is 3 and the bandwidth of  $dd$  is 0.1,  $MDE_d$  and  $MDE_c$  almost overlap each other. Thus, taking  $x = 3$  and  $dd = 0.1$  can be considered as sufficient for reliable calculation of MDE while testing the performance of a candidate GMPE. We also conducted numerous other case studies for various  $\mu_D - \sigma_D$  pairs and they did not change the major observations presented in Table 1. Therefore, choosing  $x > 3$  to cover a larger ground-motion estimation range or taking  $dd < 0.1$  for a better approximation of

continuous probability distribution of  $D$  will only increase the computational burden but will not result in improvements in the computed MDE.

We also conducted sensitivity analyses by generating synthetic ground-motion datasets to observe the variations in MDE when the intricate relation between the distributions of ground-motion datasets and GMPE estimations are of concern. These sensitivity analyses indicated that the median and standard deviation of ground-motion model estimations play a significant role on MDE values. Based on our sensitivity analyses, we determine that the index varies between 0.5 and 3.2 depending on the consistency of above two parameters with the overall trend and scatter of the observed ground-motion dataset. Details of discussions on the results of sensitivity analyses are given in Appendix A. Given two GMPEs, the MDE index computed for the small-sigma predictive model will always be smaller with respect to the other, provided that the median estimations of these GMPEs follow similar patterns. The theoretical proof of this assertion is given in Appendix B.

**Table 1**

Comparison of Modified Euclidean Distance (MDE) Values for Discrete and Continuous Probability Distributions by Considering the Variations in Bandwidths ( $dd$ ) and Number of Sigma ( $x$ )

$x$	MDE <sub>d</sub> <sup>*</sup>			MDE <sub>c</sub> <sup>†</sup>
	$dd = 0.1$	$dd = 0.05$	$dd = 0.01$	
3	0.7754	0.7762	0.7761	0.7761
4	0.7796	0.7793	0.7792	0.7792
6	0.7797	0.7794	0.7793	0.7793
8	0.7797	0.7794	0.7793	0.7793

<sup>\*</sup>MDE<sub>d</sub>: MDE values for discrete probability (calculated from equation 6)

<sup>†</sup>MDE<sub>c</sub>: MDE values for continuous probability (calculated from equation 7)

Consideration of Trend between Observed and Estimated Data: Model Bias

A significant trend between the observed data and corresponding median estimations can be interpreted as the

biased representation of the ground-motion data by the candidate predictive model. In our method, we introduce the  $\kappa$  parameter (equation 9a) to measure the level of bias between the observed and estimated data. Unlike MDE, this parameter should be computed using the entire ground-motion database. The  $\kappa$  parameter is the ratio of original ( $DE_{\text{original}}$ ) and corrected ( $DE_{\text{corrected}}$ ) Euclidean distances that are given in equations (9b) and (9c). We note that the squared Euclidean distances in equations (9b) and (9c) are equivalent to the sums of the squared residuals:

$$\kappa = \frac{DE_{\text{original}}}{DE_{\text{corrected}}} \quad (9a)$$

$$DE_{\text{original}}^2 = \sum_{i=1}^N (a_i - Y_i)^2 \quad (9b)$$

$$DE_{\text{corrected}}^2 = \sum_{i=1}^N (a_i - Y_{c,i})^2. \quad (9c)$$

In the above equations,  $a_i$  and  $Y_i$  are the natural logarithms of the  $i$ th observed and estimated data, respectively.  $N$  denotes the total data number in the assembled ground-motion database. The parameter  $Y_{c,i}$  stands for the corrected estimation of the  $i$ th data after modifying  $Y_i$  with the straight line fitted on the logarithms of the estimated and observed data. Equation (10) shows the calculation of  $Y_{c,i}$ :


$$Y_{c,i} = Y_i - (Y_{\text{fit},i} - a_i), \quad (10)$$

where  $Y_{\text{fit},i}$  is the predicted value from the regression of  $Y_i$  on  $a_i$ .

We note that the optimum value of  $\kappa$  is 1.0, and it occurs when estimations assume very close values to the corresponding observations. Illustrations for the computation of  $\kappa$  for two representative predictive models (Models 1 and 2) are given in Figure 4. The  $\kappa$  values of the example cases in Figure 4 are 1.18 and 3.41 for Models 1 and 2, respectively. As inferred from the panels on the left in this figure,  $\kappa$  increases when the trend in the fitted straight line on  $a_i$  versus  $Y_i$  becomes more noticeable, which indicates the dominant bias in the estimations of the considered GMPE (Model 2 for the cases given in Fig. 4). In our ranking method,  $\kappa$  penalizes the predictive model by comparing the  $DE$  values obtained from original and corrected residual trends. The overall calculation of EDR index is described in the subsequent section.

#### Final Form of the EDR Index and Its Use in Ground-Motion Logic-Tree Applications

The calculations presented for a single data point while describing MDE should be repeated for the entire ground-motion database as the EDR index must represent the overall probability of the differences between the estimated and observed data. This probability should then be modified by  $\kappa$  to

penalize the considered predictive model according to the level of bias detected between the median estimations and overall trend in observed data. To eliminate the dependency of EDR results on data size, the compound effect of  $\kappa$  and MDE should be normalized by the total data number,  $N$ , in the ground-motion dataset. Equation (11) shows the mathematical expression of EDR. We note that EDR index is the square root of the expression given in equation (11). A smaller EDR value implies better representation of the ground-motion dataset by the predictive model. A computer program for calculating the EDR index is available in the  electronic supplement to this article:

$$\text{EDR}^2 = \kappa \times \frac{1}{N} \times \sum_{i=1}^N \text{MDE}_i^2. \quad (11)$$

#### Implementation of EDR: Influence of $\kappa$ and MDE on the Ranking of GMPEs

Our main emphasis to this point has been the consideration of sigma (aleatory variability) and detection of model bias on the overall observed data for the optimum ranking of candidate GMPEs. This section presents a case study to show

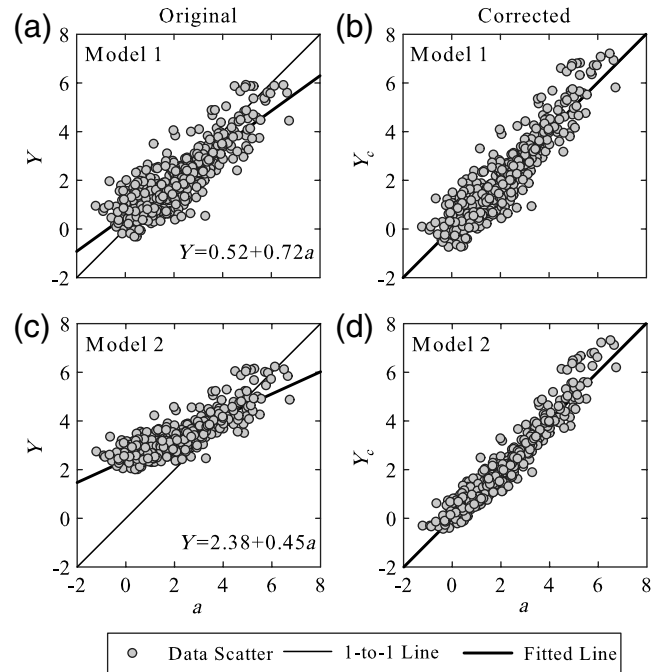


**Figure 4.** Original scatter plots of the natural logarithms of observed data,  $a$ , and corresponding median estimations,  $Y$ , obtained from Models 1 and 2 (panels [a] and [c], respectively). These scatter plots also show thick straight lines fitted on the logarithms of observed and estimated data (their equations are given on the lower right corner of each plot). Panels (b) and (d) show the relationship between the corrected median estimations ( $Y_c$ ) and observed data for Models 1 and 2, respectively. Corrected estimations of each model are calculated by using the corresponding straight-line fits given on the panels (a) and (c). The  $\kappa$  value for each model is the ratio of DE values computed from original and corrected median estimations.

how the proposed procedure accounts for these two components separately while ranking the predictive models. The case study uses an empirical ground-motion dataset compiled for ground-motion model selection and ranking under the framework of the EMME project. The database is comprised of 1703 horizontal-component accelerograms from active shallow crustal regions of Turkey (984 records), Iran (602 records), Caucasus (100 records), Jordan (6 records), and Pakistan (11 records). The moment magnitude ( $M_w$ ) versus Joyner–Boore distance ( $R_{JB}$ ; closest distance to the surface projection of fault rupture) scatter plots of the database employed in terms of country, style-of-faulting, and site class distributions are given in Figure 5. The information revealed from the scatter diagrams in Figure 5 indicates that Turkey and Iran are the major data providers to our database. The dominant rupture mechanism is strike-slip (SS) that is followed by reverse (R) and normal (N) fault events. The number of reverse and normal style-of-faulting accelerograms is close to each other, but strike-slip recordings are approximately equal to the total number of normal and reverse faulting data. Accelerograms of B and C soil categories according to Eurocode 8 (EC8; CEN, 2004) site classification dominate the site conditions. Notwithstanding, there are quite a few accelerograms (14% of total data) satisfying rock conditions (described as site class A in EC8) in the database. Almost 95% of the accelerograms pertain to events with hypocentral depths less than 30 km as shown in Figure 6. Events with hypocentral depths greater than 30 km (up to 60 km) are located either in eastern Turkey or various parts of Iran. None of the deep events from Iran fall into the Makran region, the seismotectonic settings of which generate subduction-type earthquakes (Engdahl *et al.*, 2006). The event- and record-based information of the database was compiled from vari-

ous local and international sources that are listed in Table 2. Style-of-faulting and important fault-rupture geometries of almost all events were determined from double-couple fault solutions that are mainly retrieved from global centroid moment tensor (GCMT) solutions of Harvard (see [Data and Resources](#)). To this end, we can advocate that the computed extended-source distance metrics (i.e.,  $R_{JB}$  and  $R_{RUP}$ : closest distance to the ruptured fault surface) are fairly reliable. This feature of our database is important because most of the recent GMPEs make use of extended-source distance measures while describing the variation of ground-motion amplitude as a function of source-to-site distance. We implemented a uniform data processing procedure that is based on fourth-order acausal Butterworth band-pass filtering. The high-pass and low-pass filter cutoff values were mainly identified by following the discussions in Akkar and Bommer (2006) and Akkar *et al.* (2011).

The candidate GMPEs for testing are derived for shallow active crustal regions. They are compiled from ground-motion models that are developed either from local databases or from datasets that are comprised of accelerograms from multiple countries or regions. The latter ground-motion models are denoted as global predictive models among the model developers. Figure 7 presents the country-based distributions of ground-motion datasets used in developing the candidate GMPEs considered in our study. As it can be inferred from these statistics, global models mainly contain data from one or two countries or regions. The selected GMPEs satisfy the Cotton *et al.* (2006) criteria that set *a priori* rules to preserve a certain level of quality control on the selected GMPEs. These criteria are further improved by Bommer *et al.* (2010), but we did not use them in order to avoid limiting the number of candidate GMPEs. We note that the GMPEs developed by

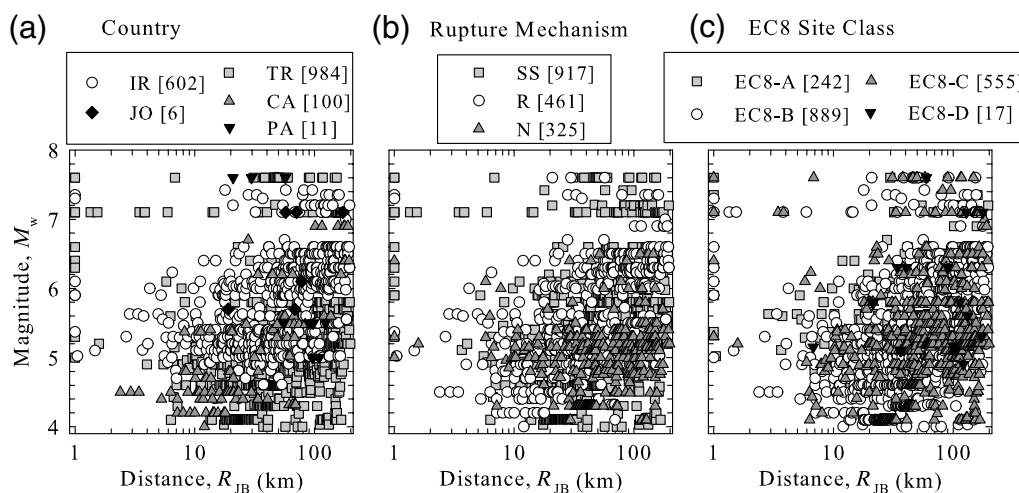


**Figure 5.** Magnitude ( $M_w$ ) versus Joyner–Boore distance ( $R_{JB}$ ) scatter plots of the considered database in terms of (a) country, (b) rupture mechanism, and (c) site class distributions. Eurocode 8 (EC8; CEN, 2004) site classification is adopted for soil definitions: site classes A, B, C, and D refer to  $V_{530}$  (average shear velocity in the upper 30 m of the soil profile) intervals of  $V_{530} \geq 800$  m/s,  $360$  m/s  $\leq V_{530} < 800$  m/s,  $180$  m/s  $\leq V_{530} < 360$  m/s, and  $V_{530} < 180$  m/s, respectively. Country or region abbreviations TR, IR, CA, JO, and PA stand for Turkey, Iran, Caucasus, Jordan, and Pakistan, respectively. The abbreviations SS, R, and N denote strike-slip, reverse, and normal style-of-faulting in the middle panel. Numeric values next to each legend describe the number of data in that group.



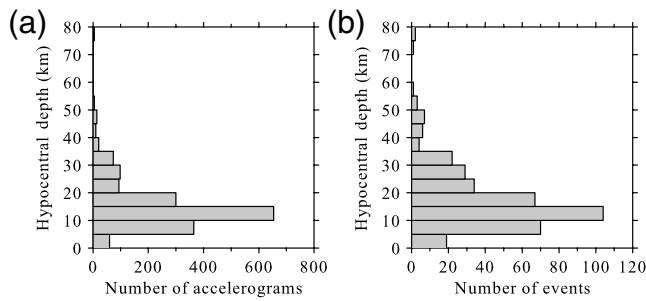


**Figure 6.** Hypocentral depth distributions in terms of (a) accelerograms and (b) earthquakes.

Zhao *et al.* (2006) and Ambraseys *et al.* (2005) do not fully comply with the Cotton *et al.* (2006) criteria. Zhao *et al.* (2006) lack the complete documentation of their model and ground-motion dataset. The model developed by Ambraseys *et al.* (2005) is recently superseded by the GMPE published in Akkar and Bommer (2010). We did not disregard these two GMPEs because they were evaluated in other regional hazard studies (e.g., Delavaud, Cotton, *et al.*, 2012). The important features of the 14 selected GMPEs are listed in Table 3. Most of these GMPEs use extended-source distance measures in their functional forms. Their  $M_w$  range generally varies between 5 and 7.5. They are devised for estimating PGA and 5%-damped pseudospectral acceleration (PSA). The selected ground-motion models generally account for major rupture mechanisms and their soil amplification terms are either continuous functions of  $V_{S30}$  or they make use of generic site definitions via dummy variables. The selected GMPEs use different horizontal component definitions, most of which are geometric mean (GM) or rotation independent average horizontal components (GMRotI50 defined in Boore *et al.*,

2006). We used the original source-to-site distance, site class, and horizontal component definition of each ground-motion model while testing their performance. We overruled this approach for GMPEs that use GMRotI50 and treated their ground-motion estimations as GM because, on average, the predicted ground motions from these two horizontal component definitions do not differ from each other (Beyer and Bommer, 2006). We note that while computing the ground-motion estimations of NGA GMPEs we used the software developed by D. M. Boore (one of the bi-products of Kaklamanos *et al.*, 2010 report and Kaklamanos *et al.*, 2011 paper). While testing the selected GMPEs, we utilized the entire database without considering the magnitude and distance limitations imposed by each ground-motion model. The general practice in many PSHA studies requires the extrapolation of GMPEs outside of their magnitude and distance ranges as few predictive models can satisfy all the magnitude and distance constraints imposed by each specific project. This fact is the major motivation behind the above decision and it is also implemented by other studies (e.g., Arango *et al.*, 2012; Delavaud, Cotton, *et al.*, 2012).

Figure 8 shows the testing results of candidate GMPEs for a spectral period band ranging from  $T = 0.0$  s (PGA) to  $T = 2.0$  s. We used eight discrete period values (i.e.,  $T = 0.0, 0.1, 0.2, 0.5, 0.75, 1.0, 1.5,$  and  $2.0$  s) within this period band in order to fully understand the performance of each candidate model under the assembled ground-motion database. Figure 8a,b shows the components of EDR index separately (i.e.,  $\sqrt{\frac{1}{N} \sum_{i=1}^N \text{MDE}_i^2}$  and  $\sqrt{\kappa}$ ) to understand the significance of sigma (ground-motion uncertainty) and agreement between the median estimations and overall data trend (model bias) for the general performance of each

**Table 2**  
Major Information Sources for Each Country-Based Strong-Motion Data (see also Data and Resources)

Database Country	Sources of Strong-Motion Data*	Catalog References†	Sources of Fault Plane Solutions‡
Turkey	AFAD ESMD IERREWS	Akkar <i>et al.</i> (2010), Sandikkaya <i>et al.</i> (2010), Erdik <i>et al.</i> (2003), Harmandar (2009)	Akkar <i>et al.</i> (2010), NEMC
Iran	ISMN ESMD	EMME and SHARE progress reports (2011)	Ghasemi <i>et al.</i> (2009), GCMT
Caucasus	GNAS NSSPRA ESMD	EMME and SHARE progress reports (2011)	WSM, GCMT
Pakistan	PMD WAPDA MSSP	EMME progress report (2011)	GCMT
Jordan	JSO	EMME progress report (2011)	GCMT

\*AFAD, Disaster and Emergency Management Presidency; ESMD, European Strong-Motion Data; GNAS, Georgian National Academy of Sciences; IERREWS, Istanbul Earthquake Rapid Response and Early Warning System; ISMN, Iran Strong Motion Network; JSO, Jordan Seismological Observatory; MSSP, Micro Seismic Study Project under Pakistan Atomic Energy Commission; NSSPRA, National Survey for Seismic Protection under the Government of the Republic of Armenia; PMD, Pakistan Meteorological Department; WAPDA, Pakistan Water and Power Development Authority

†EMME, Earthquake Model of the Middle East Region project; SHARE, Seismic Hazard HARMonization in Europe project

‡GCMT, Global Centroid Moment Tensor; NEMC, National Earthquake Monitoring Centre; WSM, World Stress Map Project

candidate GMPE. The final panel on this figure, Figure 8c, displays the product of these two components: the actual EDR index. Table 4 presents a similar type of information as Figure 8. This table lists the average values of EDR components, as well as the average EDR value computed for each predictive model over the entire period range of interest. The immediate observation from Figure 8 and Table 4 is that given the ground-motion database the performance of GMPEs shows differences in terms of addressing the aleatory variability and model bias. For example, AB10 and Zetal06, as well as CF08 and CY08, perform better while addressing the aleatory variability for the considered strong-motion database. The ground-motion models Betal10, AC10, AB10, and CF08 better represent the general trend of the observed data with respect to other candidate GMPEs. When the influence of these two factors is considered together, the method favors the performances of AB10, Zetal06, AC10, and Betal10. We believe that these observations are important since PSHA studies can follow different strategies depending on the specific objectives of each project. For example, site-specific hazard projects may prefer separate considerations of sigma influence and success of GMPEs in estimating reasonable median ground motions. To this end, such projects may design two GMPE logic trees having different sets of GMPEs that perform better in median ground-motion estimations and sigma. Separate considerations of MDE and  $\kappa$  indices may be useful for objective-specific hazard studies. In particular, MDE would provide valuable information in site-specific hazard studies if the concern is very long return periods (e.g.,  $T_R > 2500$  years). It could also be speculated that the overall EDR index can be more favorable to identify the most suitable set of GMPEs for regional hazard studies because fairly better performance of GMPEs in representing the overall data trend and aleatory variability may yield more realistic hazard results for return periods that are of interest by regional hazard programs (e.g.,  $T_R \leq 2500$  years). In passing, we note that a separate regional project (SHARE) designed the ground-motion logic tree for PSHA by selecting AB10, Zetal06, CY08, and CF08 that are also listed among

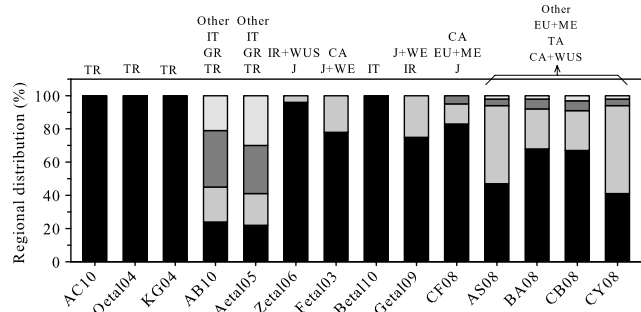


**Figure 7.** Countries or regions contributing to the databases used in the development of candidate GMPEs tested in this study: CA, California; EU, Europe; GR, Greece; IR, Iran; IT, Italy; J, Japan; ME, Middle East; TA, Taiwan; TR, Turkey; WE, West Eurasia; and WUS, western United States.

the top-ranked GMPEs in our study (see details in Delavaud, Cotton, *et al.*, 2012 for SHARE GMPE logic tree). The SHARE project proposed these GMPEs by a two-step approach that is composed of expert elicitation and model evaluation through LLH methodology. The ground-motion dataset used in SHARE is different than the one used in our paper, which may suggest the proximity of LLH and EDR methods, even if they differ conceptually. The other important observation to note is the effectiveness of statistical tools (such as EDR or LLH) in providing valuable supplementary information to hazard experts while deciding on the most suitable predictive models for the specific purposes of PSHA studies.

Another interesting observation from the testing results is the relatively better performance of GMPEs with simpler functional forms (i.e., predictive models containing the most basic estimator parameters to describe the effects of source, path, site, and rupture mechanism). Examples to such simple-format GMPEs are AB10, AC10, CF08, or Zetal06. We believe that the metadata of the basic estimator parameters used by these GMPEs was elaborated in a careful manner prior to their complete development. In other words, their strong-motion databases (either local or global) can be considered as reliable in that sense. The reliability of metadata information is important, and if it is inconsistent (or rather outdated), then predictive models can yield lower performance even if their functional forms are simpler. Typical examples to this case are KG04 (derived from an older version of the Turkish strong-motion database, which is recently updated as documented in Akkar *et al.*, 2010) and Fetal03 (whose metadata information for the same events features inconsistencies with the database used in this study that is compiled from the most recent seismological information). Ground-motion models of complex functional forms (more complicated NGA models such as AS08, CB08, and CY08) require reasonable assumptions (such as those suggested in Kaklamanos *et al.*, 2011) for most of their estimator parameters. This additional effort is necessary since the current strong-motion databases, even if they are assembled after significant efforts, would not contain all the required metadata information for the consistent execution of such GMPEs. Thus, the testing methods would not be able to acknowledge the merits of such complicated models unless the ground-motion and seismic-source information is determined in all details for the study area. Kaklamanos and Baise (2011) drew the same conclusion on the model-complexity versus model-performance stating that the more complicated NGA models do not have a predictive improvement over those of the simpler. Our experience in strong-motion database and earthquake catalog compilation suggests that the state of seismological knowledge in many seismic-prone regions is currently insufficient for the effective use of complex GMPEs. However, this comment is not meant to discourage the use or development of such high-quality GMPEs. On the contrary, we fully support the seismological community in conducting long-term research to improve the metadata information for developing

**Table 3**  
General Features of Considered Ground-Motion Prediction Equations (GMPEs)

GMPE	GMPE Acronym	Main Region(s)	Number of Records and Events	Numbers of Estimators	$M_w$ Interval	$R$ Type and $R_{max}$ (km) *	Component †	Style-of-Faulting ‡	Site Effect
Akkar and Çağnan (2010)	AC10	Turkey	433, 137	4	5.0–7.6	$R_{JB}$ : 200	PGA, PGV, PSA in GM	SS, N, R	$V_{S30}$
Özbey <i>et al.</i> (2004)	Oeta104	Northwestern Turkey	195, 17	3	5.0–7.4	$R_{JB}$ : 300	PGA, PSA in GM	U	Dummy variable
Kalkan and Gülkan (2004)	KG04	Turkey	112, 57	3	4.0–7.4	$R_{JB}$ : 250	PGA, PSA in L	U	$V_{S30}$
Akkar and Bommer (2010)	AB10	Europe and the Middle East	532, 131	4	5.0–7.6	$R_{JB}$ : 100	PGA, PGV, PSA in GM	SS, N, R	Dummy variable
Ambraseys <i>et al.</i> (2005)	Aeta105	Europe and the Middle East	595, 135	4	5.0–7.6	$R_{JB}$ : 99	PGA, PSA in L	SS, N, T, O	Dummy variable
Zhao <i>et al.</i> (2006)	Zeta106	Japan	4726, 269	5	5.0–8.3	$R_{RUP}$ : 300	PGA, PSA in GM	SS, N, R	Dummy variable
Fukushima <i>et al.</i> (2003)	Feta103	West Eurasia	740, 50	3	5.5–7.4	$R_{RUP}$ and $R_{HYP}$ : 235	PGA, PSA in B	U	Dummy variable
Bindi <i>et al.</i> (2010)	Beta110	Italy	561, 107	3	4.0–6.9	$R_{JB}$ and $R_{EPI}$ : 100	PGA, PGV, PSA in L	U	Dummy variable
Ghasemi <i>et al.</i> (2009)	Getal09	Iran	716, 200	3	5.0–7.4	$R_{RUP}$ and $R_{HYP}$ : 100	PGA, PGV, PSA in V	U	Dummy variable
Cauzzi and Faccioli (2008)	CF08	Japan	1164, 60	4	5.0–7.2	$R_{HYP}$ : 150	PSA in GMRot50	SS, N, R	Dummy variable
Faccioli <i>et al.</i> (2010)	AS08	Western U.S. and Taiwan	2754, 135	13	5.0–8.5	$R_{RUP}$ : 200	PGA, PGV, PSA in GMRot50	SS, N, R	$V_{S30}$
Boore and Atkinson (2008)	BA08	Western U.S. and Taiwan	1574, 58	5	5.0–8.0	$R_{JB}$ : 200	PGA, PGV, PSA in GMRot50	SS, N, R	$V_{S30}$
Campbell and Bozorgnia (2008)	CB08	Western U.S. and Taiwan	1561, 64	9	4.0–8.5	$R_{RUP}$ : 200	PGA, PGV, PSA in GMRot50	SS, N, R	$V_{S30}$
Chiou and Youngs (2008)	CY08	Western US and Taiwan	1950, 125	12	4.0–8.5	$R_{RUP}$ : 200	PGA, PGV, PSA in GMRot50	SS, N, R	$V_{S30}$

\* $R$ : distance,  $R_{max}$ : maximum distance,  $R_{EPI}$ : epicentral distance,  $R_{HYP}$ : hypocentral distance,  $R_{JB}$ : Joyner-Boore distance,  $R_{RUP}$ : closest distance

†GM, geometric mean of horizontal components; L, larger horizontal component; GMRot50, rotation-independent average horizontal component (Boore *et al.*, 2006); B, both horizontal components; V, vertical component

‡SS, strike-slip faulting; N, normal faulting; R, reverse faulting; O, oblique faulting; U, unidentified

well-constrained GMPEs to better address the contribution of source, path, and site effects in hazard estimations.

### Summary and Conclusions

In this paper, we propose an alternative testing procedure for testing and ranking of GMPEs that can be used for designing GMPE logic trees in PSHA studies. The method is based on the Euclidean distance concept that carries similar features with the conventional residual analysis. The method can be a useful guide to build ground-motion logic trees from properly ranked GMPEs, if it is used together with other well-designed testing methods, as well as visual tools, such as residual analysis.

The proposed procedure accounts for aleatory variability in ground-motion estimations (through standard deviations of GMPEs). It also considers the bias between median estimations and observed ground-motion data (model bias). The bias between median ground-motion estimations and general variation of observed data is identified by the  $\kappa$  parameter, which makes an analogy to the residual analysis

concept. The uncertainty in ground-motion variability is addressed by finding the probability distribution of the differences between the observed data and corresponding estimations for a range of sigma values. This approach differs from that which was employed in the LLH method (Scheraum *et al.*, 2009) because LLH computes the occurrence probability of the observed data point by using the corresponding estimation that is assumed to be log-normally distributed with median and sigma values of the candidate GMPE.

We presented a case study to illustrate the general features of the proposed procedure using a database that is compiled from the shallow active crustal recordings of the Middle East, Caucasus, and Pakistan. We selected 14 GMPEs for the presented case study that are suitable for estimating the ground-motion intensities of seismotectonic features mimicked by the strong-motion database. The results of the case study suggest that the aleatory variability (i.e., sigma) and the bias between median estimations and observed ground-motion data (model bias) play separate roles in the performance of GMPEs to properly represent the selected ground-motion dataset. Our procedure is capable of providing this useful information to the seismic hazard expert. Such information can be used in various ways to establish the GMPE logic tree depending on the objective of the hazard project, which can be either forecasting the regional or site-specific hazard. The case study also indicated that GMPEs having simpler functional forms rank better than those whose predictive equations contain complex estimator parameters. If the metadata of the strong-motion database lacks information about these estimator parameters, they should be computed by making reasonable assumptions. However,

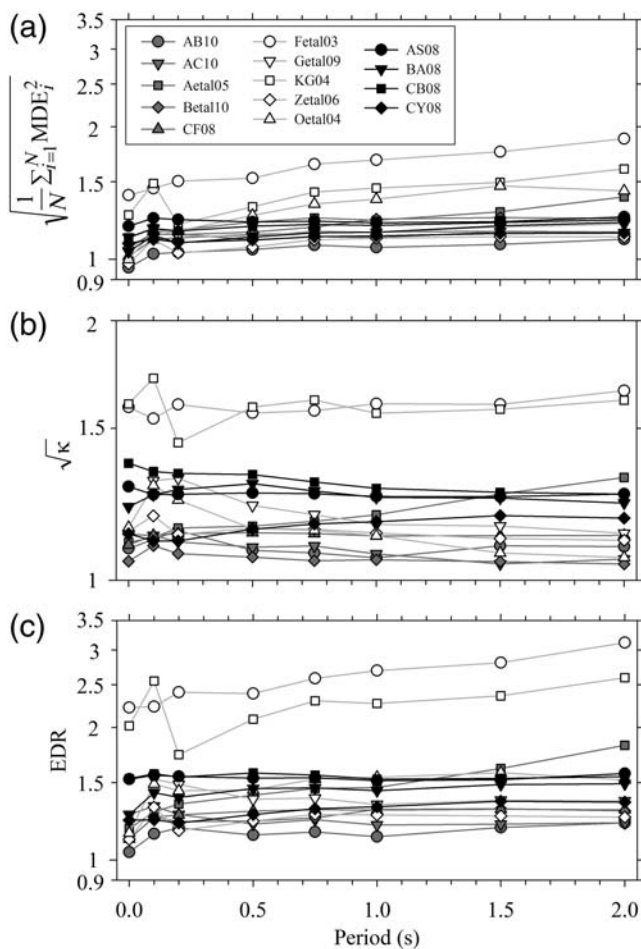


**Figure 8.** Separate EDR components: (a)  $\sqrt{\frac{1}{N} \sum_{i=1}^N MDE_i^2}$ , (b)  $\sqrt{\kappa}$ , and (c) the actual EDR index.

Table 4

Performance of Tested Ground-Motion Prediction Equations (GMPEs) for each Individual Component of Euclidean Distance-Based Ranking (EDR), As Well As the EDR Index

GMPEs	$\sqrt{\frac{1}{N} \sum_{i=1}^N MDE_i^2}$	$\sqrt{\kappa}$	EDR
AB10	<b>1.05</b>	<b>1.10</b>	<b>1.15</b>
AC10	1.14	<b>1.09</b>	<b>1.24</b>
Aetal05	1.22	1.19	1.45
AS08	1.22	1.26	1.54
BA08	1.14	1.25	1.42
Betal10	1.17	<b>1.06</b>	<b>1.25</b>
CB08	1.18	1.31	1.55
CF08	<b>1.12</b>	<b>1.13</b>	1.27
CY08	<b>1.12</b>	1.15	1.29
Fetal03	1.60	1.59	2.55
Getal09	1.16	1.21	1.41
KG04	1.40	1.59	2.24
Oetal04	1.27	1.16	1.46
Zetal06	<b>1.08</b>	1.14	<b>1.23</b>

The reported indices are the averages over spectral ordinates of selected period range. The top four best performing models are shown in bold.

no matter how reasonable these assumptions are, they impose additional uncertainty to the estimations of such complicated GMPEs that, in turn, affects their performances.

### Data and Resources

This study uses the ground-motion database compiled for the EMME project. The strong ground-motion data in the EMME database is obtained from the following sources: AFAD at [http://daphne.deprem.gov.tr/2K/daphne\\_v4.php](http://daphne.deprem.gov.tr/2K/daphne_v4.php), ESMD at [www.isesd.hi.is/ESD\\_Local/frameaset.htm](http://www.isesd.hi.is/ESD_Local/frameaset.htm), IERREWS at [http://www.koeri.boun.edu.tr/Research/Early\\_WarnIng\\_System\\_13\\_139.depmuh](http://www.koeri.boun.edu.tr/Research/Early_WarnIng_System_13_139.depmuh), ISMN at [www.bhrc.ac.ir/portal/Default.aspx?tabid=635](http://www.bhrc.ac.ir/portal/Default.aspx?tabid=635), GNAS at [www.science.org.ge/english.html](http://www.science.org.ge/english.html), NSSPRA at [www.adrc.asia/highlights/041/nsspra.htm](http://www.adrc.asia/highlights/041/nsspra.htm), PMD at [www.pmd.gov.pk/](http://www.pmd.gov.pk/), WAPDA at [www.wapda.gov.pk/htmls/auth-index.html](http://www.wapda.gov.pk/htmls/auth-index.html), MSSP at [www.paec.gov.pk/](http://www.paec.gov.pk/), JSO at [www.nra.gov.jo/index.php?option=com\\_content&task=view&id=83&Itemid=122](http://www.nra.gov.jo/index.php?option=com_content&task=view&id=83&Itemid=122) (all were last accessed August 2012).

The catalog (metadata) information of the recordings in the database is retrieved from sources of Erdik *et al.* (2003), Harmandar (2009), Akkar *et al.* (2010), and Sandikkaya *et al.* (2010), and EMME and SHARE progress reports (2011) at <http://emme-gem.org/>, and [www.share-eu.org/](http://www.share-eu.org/), respectively (all websites were last accessed August 2012). The main sources for the double-couple fault plane solutions are Ghasemi *et al.* (2009), Akkar *et al.* (2010), GCMT at [www.globalcmt.org/](http://www.globalcmt.org/), NEMC at [www.koeri.boun.edu.tr/sismo/indexeng.htm](http://www.koeri.boun.edu.tr/sismo/indexeng.htm), and WSM at <http://dc-app3-14.gfz-potsdam.de/> (all websites were last accessed August 2012).

The software that computes the ground-motion estimations of NGA GMPEs was obtained from the website of D. M. Boore at [www.daveboore.com/](http://www.daveboore.com/) (last accessed August 2012).

### Acknowledgments

The work presented in this paper has been developed within the EMME project funded by the Global Earthquake Model (GEM) organization. Professors Ayşen Akkaya and Tolga Yılmaz of the Middle East Technical University (METU), as well as Laurentiu Danciu of the Eidgenössische Technische Hochschule Zurich (ETH, Zurich), contributed with valuable feedback during the development of the proposed procedure. The constructive and detailed comments of Elise Delavaud and James Kaklamanos significantly improved the technical nature of the paper.

### References

- Abrahamson, N., and W. Silva (2008). Summary of the Abrahamson & Silva NGA ground-motion relations, *Earthq. Spectra* **24**, no. 1, 67–97.
- Akkar, S., and J. J. Bommer (2006). Influence of long-period filter cut-off on elastic spectral displacements, *Earthq. Eng. Struct. Dynam.* **35**, no. 9, 1145–1165.
- Akkar, S., and J. J. Bommer (2010). Empirical equations for the prediction of PGA, PGV, and spectral accelerations in Europe, the Mediterranean region, and the Middle East, *Seismol. Res. Lett.* **81**, no. 2, 195–206.
- Akkar, S., and Z. Çağnan (2010). A local ground-motion predictive model for Turkey and its comparison with other regional and global ground-motion models, *Bull. Seismol. Soc. Am.* **100**, no. 6, 2978–2995.
- Akkar, S., Z. Çağnan, E. Yenier, Ö. Erdoğan, M. A. Sandikkaya, and P. Gülkan (2010). The recently compiled Turkish strong motion database: Preliminary investigation for seismological parameters, *J. Seismol.* **14**, 457–479.
- Akkar, S., Ö. Kale, E. Yenier, and J. J. Bommer (2011). The high-frequency limit of usable response spectral ordinates from filtered analogue and digital strong-motion accelerograms, *Earthq. Eng. Struct. Dynam.* **40**, 1387–1401.
- Ambraseys, N. N., J. Douglas, S. K. Sarma, and P. M. Smith (2005). Equations for the estimation of strong ground motions from shallow crustal earthquakes using data from Europe and the Middle East: Horizontal peak ground acceleration and spectral acceleration, *Bull. Earthq. Eng.* **3**, no. 1, 1–53.
- Arango, M. C., F. O. Strasser, J. J. Bommer, J. M. Cepeda, R. Boroschek, D. A. Hernandez, and H. Tavera (2012). An evaluation of the applicability of current ground-motion models to the South and Central American subduction zones, *Bull. Seismol. Soc. Am.* **102**, no. 1, 143–168.
- Beauval, C., F. Cotton, N. Abrahamson, N. Theodoulidis, E. Delavaud, L. Rodriguez, F. Scherbaum, and A. Haendel (2012b). Regional differences in subduction ground motions, in *Proceedings of the 15th World Conference on Earthquake Engineering*, Lisbon, Portugal, 24–28 September 2012.
- Beauval, C., H. Tasan, A. Laurendeau, E. Delavaud, F. Cotton, Ph. Guéguen, and N. Kühn (2012a). On the testing of ground-motion prediction equations against small magnitude data, *Bull. Seismol. Soc. Am.* **102**, no. 5, 1994–2007.
- Beyer, B., and J. J. Bommer (2006). Relationships between median values and between aleatory variabilities for different definitions of the horizontal component of motion, *Bull. Seismol. Soc. Am.* **96**, no. 4A, 1512–1522.
- Bindi, D., L. Luzi, M. Massa, and F. Pacor (2010). Horizontal and vertical ground-motion prediction equations derived from the Italian Accelerometric Archive (ITACA), *Bull. Earthq. Eng.* **8**, no. 5, 1209–1230.
- Bindi, D., L. Luzi, F. Pacor, G. Franceschina, and R. R. Castro (2006). Ground-motion predictions from empirical attenuation relationships versus recorded data: The case of the 1997–1998 Umbria–Marche, Central Italy, strong-motion dataset, *Bull. Seismol. Soc. Am.* **96**, no. 3, 984–1002.
- Bommer, J. J., J. Douglas, F. Scherbaum, F. Cotton, H. Bungum, and D. Fäh (2010). On the selection of ground-motion prediction equations for seismic hazard analysis, *Seismol. Res. Lett.* **81**, 783–793.
- Boore, D. M., and G. Atkinson (2008). Ground-motion prediction equations for the average horizontal component of PGA, PGV, and 5%-damped PSA at spectral periods between 0.01 s and 10.0 s, *Earthq. Spectra* **24**, no. 1, 99–138.
- Boore, D. M., J. Watson-Lamprey, and N. A. Abrahamson (2006). Orientation-independent measures of ground motion, *Bull. Seismol. Soc. Am.* **96**, no. 4A, 1502–1511.
- Campbell, K. W., and Y. Bozorgnia (2008). NGA ground-motion model for the geometric mean horizontal component of PGA, PGV, PGD, and 5% damped linear elastic response spectra for periods ranging from 0.01 to 10 s, *Earthq. Spectra* **24**, no. 1, 139–171.
- Cauzzi, C., and E. Faccioli (2008). Broadband (0.05–20 s) prediction of displacement response spectra based on worldwide digital records, *J. Seismol.* **12**, no. 4, 453–475.
- CEN (2004). Eurocode 8: Design of structures for earthquake Resistance—Part 1: General rules, seismic actions, and rules for buildings, EN 1998-1:2004, Comité Européen de Normalisation, Brussels, Belgium.
- Chiou, B. S.-J., and R. R. Youngs (2008). An NGA model for the average horizontal component of peak ground motion and response spectra, *Earthq. Spectra* **24**, no. 1, 173–215.
- Cotton, F., F. Scherbaum, J. J. Bommer, and H. Bungum (2006). Criteria for selecting and adjusting ground-motion models for specific target regions: Application to Central Europe and rock sites, *J. Seismol.* **10**, 137–156.

- Delavaud, E., F. Cotton, S. Akkar, F. Scherbaum, L. Danciu, C. Beauval, S. Drouet, J. Douglas, R. Basili, M. A. Sandikkaya, M. Segou, E. Faccioli, and N. Theodoulidis (2012). Toward a ground-motion logic tree for probabilistic seismic hazard assessment in Europe, *J. Seismol.* **16**, 451–473.
- Delavaud, E., F. Scherbaum, N. Kuehn, and T. Allen (2012). Testing the global applicability of ground-motion prediction equations for active shallow crustal regions, *Bull. Seismol. Soc. Am.* **102**, no. 2, 707–721.
- Delavaud, E., F. Scherbaum, N. Kuehn, and C. Riggelsen (2009). Information-theoretic selection of ground-motion prediction equations for seismic hazard analysis: An applicability study using Californian data, *Bull. Seismol. Soc. Am.* **99**, no. 6, 3248–3263.
- Devore, J. L. (2004). Probability and statistics for engineering and the sciences, Thomson Learning Inc., Massachusetts.
- Engdahl, E. R., J. A. Jackson, S. C. Myers, E. A. Bergman, and K. Priestley (2006). Relocation and assessment of seismicity in the Iran region, *Geophys. J. Int.* **167**, 761–778.
- Erdik, M., Y. Fahjan, O. Ozel, H. Alcik, A. Mert, and M. Gul (2003). Istanbul earthquake rapid response and early warning system, *Bull. Earthq. Eng.* **1**, 157–163.
- Faccioli, E., M. Villani, M. Vanini, and C. Cauzzi (2010). Mapping seismic hazard for the needs of displacement-based design: The Case of Italy, *Adv. Performance-Based Earthq. Eng.* **13**, no. 1, 3–14.
- Fukushima, Y., C. Berge-Thierry, P. Volant, D.-A. Griot-Pommer, and F. Cotton (2003). Attenuation relation for western Eurasia determined with recent near-fault records from California, Japan and Turkey, *J. Earthq. Eng.* **7**, no. 4, 573–598.
- Ghasemi, H., M. Zare, Y. Fukushima, and K. Koketsu (2009). An empirical spectral ground-motion model for Iran, *J. Seismol.* **13**, 499–515.
- Harmandar, E. (2009). Spatial variation of strong ground motion, *Ph. D. dissertation*, Bogaziçi University, İstanbul, Turkey.
- Hintersberger, E., F. Scherbaum, and S. Hainzl (2007). Update of likelihood-based ground-motion model selection for seismic hazard analysis in western central Europe, *Bull. Earthq. Eng.* **5**, 1–16.
- Kaklamanos, J., and L. G. Baise (2011). Model validations and comparisons of the next generation attenuation of ground motions (NGA–West) project, *Bull. Seismol. Soc. Am.* **101**, no. 1, 160–175.
- Kaklamanos, J., L. G. Baise, and D. M. Boore (2011). Estimating unknown input parameters when implementing the NGA ground-motion prediction equations in engineering practice, *Earthq. Spectra* **27**, 1219–1235.
- Kaklamanos, J., D. M. Boore, E. M. Thompson, and K. W. Campbell (2010). Implementation of the next generation attenuation (NGA) ground-motion prediction equations in Fortran and R, *U.S. Geol. Surv. Open-File Rept. 2010-1296*, 43 pp.
- Kalkan, E., and P. Gülkan (2004). Site-dependent spectra derived from ground-motion records in Turkey, *Earthq. Spectra* **20**, 1111–1138.
- Mousavi, M., A. Ansari, H. Zafarani, and A. Azarbakht (2012). Selection of ground motion prediction models for seismic hazard analysis in the Zagros region, Iran, *J. Earthq. Eng.* **16**, 1184–1207.
- Nash, J. E., and J. V. Sutcliffe (1970). River flow forecasting through conceptual models: Part I—A discussion of principles, *J. Hydrol.* **10**, 282–290.
- Özbey, C., A. Sari, L. Manuel, M. Erdik, and Y. Fahjan (2004). An empirical attenuation relationship for northwestern Turkey ground motion using a random effects approach, *Soil Dynam. Earthq. Eng.* **24**, no. 2, 115–125.
- Power, M., B. Chiou, N. Abrahamson, Y. Bozorgnia, T. Shantz, and C. Roblee (2008). An overview of the NGA project, *Earthq. Spectra* **24**, no. 1, 3–21.
- Restrepo-Velez, L. F., and J. J. Bommer (2003). An exploration of the nature of the scatter in ground-motion prediction equations and the implications for seismic hazard assessment, *J. Earthq. Eng.* **7**, no. S11, 171–199.
- Sandikkaya, M. A., M. T. Yılmaz, B. S. Bakır, and Ö. Yılmaz (2010). Site classification of Turkish national strong-motion stations, *J. Seismol.* **14**, 543–563.
- Scasserra, G., J. P. Stewart, P. Bazzurro, G. Lanzo, and F. Mollaioli (2009). A comparison of NGA ground-motion prediction equations to Italian data, *Bull. Seismol. Soc. Am.* **99**, no. 5, 2961–2978.
- Scherbaum, F., F. Cotton, and P. Smith (2004). On the use of response spectral-reference data for the selection and ranking of ground-motion models for seismic-hazard analysis in regions of moderate seismicity: The case of rock motion, *Bull. Seismol. Soc. Am.* **94**, no. 6, 2164–2185.
- Scherbaum, F., E. Delavaud, and C. Riggelsen (2009). Model selection in seismic hazard analysis: An information-theoretic perspective, *Bull. Seismol. Soc. Am.* **99**, no. 6, 3234–3247.
- Shoja-Taheri, J., S. Naserieh, and G. Hadi (2010). A test of the applicability of NGA models to the strong ground-motion data in the Iranian plateau, *J. Earthq. Eng.* **14**, 278–292.
- Stafford, P. J., F. O. Strasser, and J. J. Bommer (2008). An evaluation of the applicability of the NGA models to ground-motion prediction in the Euro-Mediterranean region, *Bull. Earthq. Eng.* **6**, 149–177.
- Zhao, J. X., J. Zhang, A. Asano, Y. Ohno, T. Oouchi, T. Takahashi, H. Ogawa, K. Irikura, H. K. Thio, P. G. Somerville, and Y. Fukushima (2006). Attenuation relations of strong ground motion in Japan using site classification based on predominant period, *Bull. Seismol. Soc. Am.* **96**, no. 3, 898–913.

## Appendix A

Assuming log-normal distribution, the synthetic datasets are generated for various number of data, which varies between 30 and 210, in increments of 30. The synthetics mimic the observed ground-motion datasets in these analyses. Figure A1 shows the distributions (histograms) of a sample set of synthetic datasets generated for  $\mu = 0.5$  and

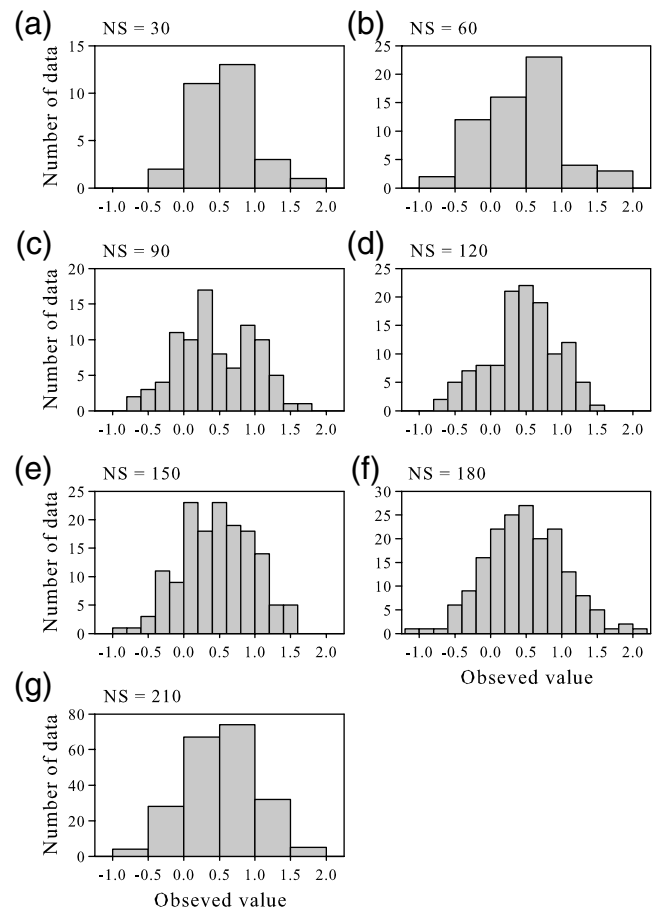


**Figure A1.** A sample set of synthetic datasets with various data sizes (NS).

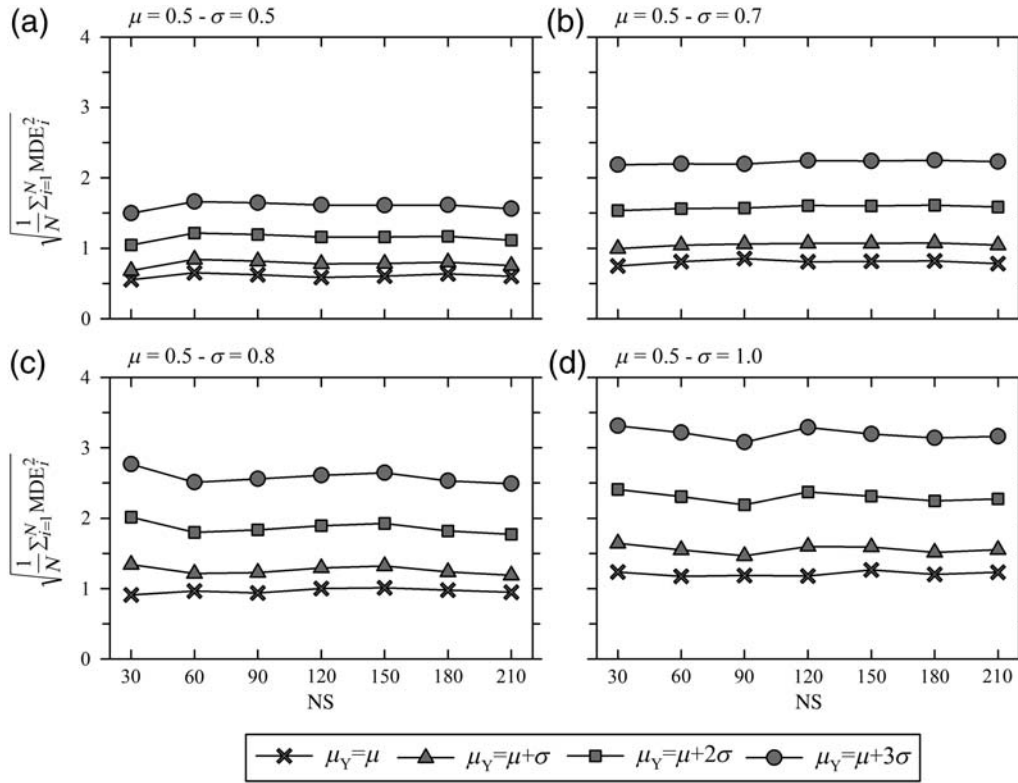


**Figure A2.** Variation of MDE (i.e.,  $\sqrt{\frac{1}{N} \sum_{i=1}^N \text{MDE}_i^2}$ ) for different scenarios in terms of ground-motion model estimations with different median ( $\mu_Y$ ) and standard deviations ( $\sigma_Y$ ), which are adjusted by considering the median ( $\mu$ ) and standard deviations ( $\sigma$ ) of generated synthetic datasets.

$\sigma = 0.5$  (median and standard deviation of the generated synthetic dataset, respectively). The synthetic data that represent the observed values are plotted in logarithmic scale in this figure.

Figure A2 shows the variations in MDE (i.e.,  $\sqrt{\frac{1}{N} \sum_{i=1}^N \text{MDE}_i^2}$ ) in terms of different sample sizes of synthetic data. The median,  $\mu$ , is taken as 0.5 in all cases whereas  $\sigma$  is varied as 0.5, 0.7, 0.8, and 1.0 while generating the synthetic data for each set. The standard deviations of model estimations ( $\sigma_Y$ ) are assumed to follow the standard deviations of the generated synthetic datasets (i.e.,  $\sigma_Y = \sigma$ ). The medians of model estimations ( $\mu_Y$ ) systematically take different values in each case. Four different  $\mu_Y$  levels are considered in the sensitivity analyses:  $\mu_Y = \mu$ ,  $\mu_Y = \mu + \sigma$ ,  $\mu_Y = \mu + 2\sigma$ , and  $\mu_Y = \mu + 3\sigma$ . The plots in Figure A2 summarize the changes in MDE for the entire sensitivity analyses by making use of above cases.

One can infer that MDE is independent of data size from the plots in Figure A2. When median and standard deviations of model estimations are very similar to the average trend and scatter of observed data (i.e.,  $\mu_Y = \mu$  and  $\sigma = \sigma_Y$ ), MDE attains values between 0.5 and 1.2 depending on the level of scatter in the observed data. In other words, as the scatter in observed data increases MDE starts to increase even if the standard deviations of model estimations follow very similar

trends to those of observed data. MDE varies between 1.5 and 3.2 when the model estimations significantly differ with respect to the observed data (i.e.,  $\mu_Y = \mu + 3\sigma$ ). The increase in MDE depends on the dispersion of observed ground-motion dataset as in the previous case.

### Appendix B

The Euclidean distance-based ranking (EDR) method selects  $|d|_{\max}$  by considering the area under the normally distributed parameter  $D$  that gives the difference between the absolute value of natural logarithms of observed and estimated data points (equation 2). The value of  $|d|_{\max}$  depends on the standard deviation of ground-motion prediction equation (GMPE) (equation 8). The probabilities of discrete  $d_j$  that are greater or less than  $|d|_{\max}$  are almost zero if the area to be considered under this probability distribution is determined as 99.7% as suggested in the paper. Figure B1 shows the normally distributed  $D$  parameters of two models having the same median estimations but different standard deviations. The standard deviation of Model 2 is greater than that of Model 1, which results in higher  $d_{\max}$  in Model 2 (i.e.,  $|d|_{\max,2} > |d|_{\max,1}$ ). As depicted in Figure B1,  $d_j$  values that are close to the medians of both models attain small values with high occurrence probabilities. The occurrence probabilities of  $d_j$  values become smaller as they begin shifting

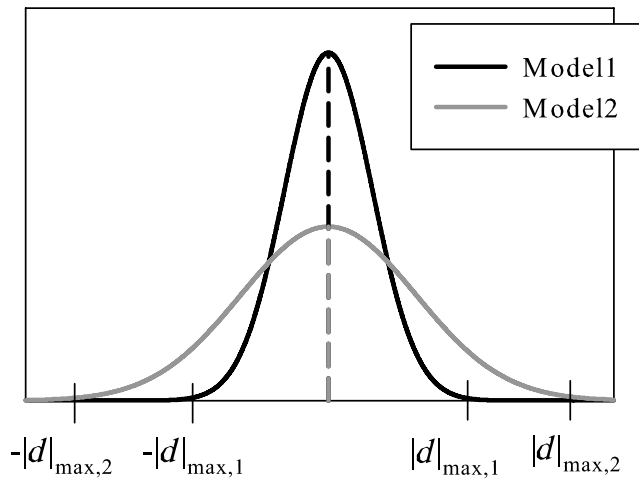


**Figure B1.** Comparisons between two ground-motion prediction equations (GMPEs) (predictive models) having the same medians and different standard deviations

away from the median. When  $d_j$  takes larger values between  $-|d|_{\max,2}$  and  $-|d|_{\max,1}$  or  $|d|_{\max,1}$  and  $|d|_{\max,2}$ , their occurrence probability is almost zero for Model 1 but is still significant for Model 2. From these discussions and the expression used for computing MDE (equation 6), one can infer that MDE value computed for Model 1 will always be smaller than that of Model 2.

Earthquake Engineering Research Center  
 Middle East Technical University  
 K6 Building  
 06800 Ankara, Turkey  
 ozkankale@gmail.com  
 sakkar@metu.edu.tr

Manuscript received 7 April 2012